Pre-Departure Planning for Urban Air Mobility Flights with Dynamic Airspace Reservation

Guodong Zhu* and Peng Wei†
Iowa State University, Ames, IA, 50011, U.S.A.

Urban Air Mobility (UAM) is new air transportation concept where highly autonomous aircraft could safely and efficiently transport passengers and cargo within the city by rising above the traffic congestion on the ground. Conflict avoidance is a core research problem to enable UAM for high density operations. As the outer layer of protection, pre-departure planning can optimize trajectory under physical and operation constraints, coordinate flights with existing flight plans, alleviate the burden of inner layer sense and avoid, and increase the predictability of an operation. Dynamic geofence is a moving region of reserved airspace for an aircraft, which provides a safety buffer for various uncertainties including flight operation, localization and disturbances from weather. This paper is an endeavor to do pre-departure conflict-free trajectory planning for flight with dynamic geofence in structured airspace. We propose an efficient, scalable, two-phase, linear programming based algorithm. In the first phase of the algorithm, we discretize the flight into time periods and formulate an integer programming model, which is proved to be Totally Unimodular (TU), to avoid conflict with already filed flight plans and to determine the location of dynamic geofence in each time period. In the second phase, we propose a velocity profile smoothing model to make the trajectory easier to fly. This main advantage of this algorithm is its verifiable safety guarantee, which can be valuable to the UAM community.

Nomenclature

Sets and Indices

$\mathcal{F}$	Set of flights, $f = 1, \cdots, \lvert\mathcal{F}\rvert$
$\mathcal{T}$	Set of time periods, $t = 1, \cdots, T$
$\mathcal{F}_f$	Set of route options for flight f, $r = 1, \cdots, \lvert\mathcal{F}_f\rvert$
$\mathcal{P}$	Set of potential collision points, $p = 1, \cdots, \lvert\mathcal{P}\rvert$
Ω_{fr}	Ordered set of indices of potential collision points which flight f crosses if taking route r, possibly empty
T^p_{fr}	Set of allowed time periods for flight f taking route r to departs from/pass through vertipad/potential collision point p
C	Set of ordered pairs of potential collision points. $(p, p') \in C$ iff p is connected to p' in the graph
Φ_p	Set of routes which cross potential collision point p
$\tilde{T}^p_{fr}$	Set of time periods for flight f taking route r to pass through potential collision point p; $\tilde{T}^p_{fr} \in T^p_{fr}$

Input Parameters

N_{fr}	Number of potential collision points along route r of flight f
$\Omega^0_{fr}, \Omega^{N_{fr}}_{fr}$	The departure vertipad and last potential collision point along route r of flight f

*Graduate Student, Aerospace Engineering Department, Iowa State University, Ames, IA, AIAA Student Member.
†Assistant Professor, Aerospace Engineering Department, Iowa State University, Ames, IA, AIAA Senior Member.

c_{fr}, c_g, c_a Cost for flight f taking route r, taking one unit of ground delay/air delay

$\underline{T}^p_{fr}$ First time period in the set T^p_{fr}

$\overline{T}^p_{fr}$ Last time period in the set T^p_{fr}

$\Delta^{p,p'}$ Number of time periods to travel from potential collision point p to p', defined for all pairs $(p, p') \in C$

M^p_t Binary indictor whether potential collision point is accessible in time period t

$d^{p,p'}$ Maximum units of delay flight can take between potential collision point p and p'

$\text{Dep}_f, \text{Arr}_f$ Scheduled departure/arrival time of flight f

L_t, R_t Front/rear end of dynamic geofence at timestamp t

o_t Optimal position of aircraft in dynamic geofence at timestamp t

$v_{\max}, v_{\min}$ Allowed maximum/minimum velocity of an eVTOL

$a_{\text{acc}}, a_{\text{dec}}$ Allowed maximum acceleration/deceleration of an eVTOL

$\dot{a}_{\max}$ Maximum allowed jitter

DG_f Dynamic geofence of flight f

Primary Decision Variables

w^{pr}_{ft} Binary indicator whether flight f taking route r with its the front end of the dynamic geofence reaching potential collision node p by time period t

$a_{\bar{t}}$ Acceleration at finer-grained timestamp $\bar{t}$

Auxiliary Variables

δ_{fr} Binary indicator whether flight f will take route r

$x_{\bar{t}}$ Location along the route at finer-grained timestamp $\bar{t}$

$v_{\bar{t}}$ Velocity along the route at finer-grained timestamp $\bar{t}$

I. Introduction

Technology advancements, especially the improvement of intelligent decision tools and distributed electric propulsion, and new business models for daily commute within an urban area have prepared an era of On-Demand Mobility (ODM) for aviation [1, 2]. Over a dozen companies including Airbus, Bell, Embraer, Volocopter and Aurora Flight Sciences are building and testing their electric Vertical Takeoff and Landing (eVTOL) aircraft to make it a reality [3]. In order to make Urban Air Mobility (UAM) profitable for air taxi operators and affordable for passengers, high density of air operations is necessary, which is beyond the current capability of traditional air traffic control service providers. As one of the industry leaders, Uber estimated that there can be more than 5,000 eVTOL flights per day in the city of Los Angeles alone for its future scaled Uber Air operations [4]. A more automated air traffic control system is much needed to ensure safe and efficient UAM operations [5, 6].

There has been a growing number of research on automated conflict detection and resolution, arrival and departure management and weather avoidance for high-altitude airspace management, represented by the work from NASA [7–9]. Recently, this effort has been extended to UAM application [10]. Researchers have been applying various frameworks to solve conflict avoidance problem. Other representative work includes geometry based approach [11], (nonlinear) optimization based approach [12], Markov Decision Process based approach [13], Monte Carlo tree search based approach [14], and Deep Reinforcement Learning based approach [15].

Pre-departure planning is an important stage for commercial airliner operations, and we believe it will continue being a key component in UAM network scheduler. There are several important roles pre-departure planning can play.

For example, it helps a flight to avoid weather impacted airspace, no-fly zones or severely congested regions. Serving as the outer layer of protection, it can coordinate a flight with existing filed flight plans to minimize potential conflicts, thus minimizing the stress of inner layer sense and avoid system. It can also give a common situation awareness (aircraft location, velocity, route and flight duration, etc) to airspace participators.

Dynamic geofence is a promising concept for low-altitude flight operation and has been studied in the context of Unmanned Aerial System (UAS) Traffic Management (UTM) [16–18]. The key idea of dynamic geofence is that it is a moving region of reserved airspace for an aircraft, which provides a buffer for various uncertainties including flight operation, localization, wind and approximation errors from discretization. Dynamic geofence can be considered as an extension of the minimum separation requirement imposed by the Federal Aviation Administration (FAA) [19].

The goal of this paper is to plan conflict-free trajectory for flight with dynamic geofence. This work is the continuation of our previous pre-departure coordination paper [16]. We still plan the trajectory on structured airspace, since more and more research endorses that structured airspace works better than free-fly concept for high density UTM operations [20, 21]. Compared with [16], this work is more flexible, since it now allows aircraft to take ground delay, perform speed adjustment and reroute. It is also less conservative, since the calculation and estimation of dynamic geofence location are no longer based on extreme aircraft performance. Compared with NASA's outstanding work [10], which could also do pre-departure conflict resolutions, we believe there are three advantages of our approach:

1) it does not rely on sophisticated in-house simulation software and can still give key decisions and capture the tradeoffs between ground and air delay (speed change) and reroute/maneuver
2) it does not optimize resolution for conflict one after another, instead it optimizes all resolutions at the same time, and thus achieves "global" optimum
3) with dynamic geofence, in the first phase of algorithm, we can get a robust solution for various uncertainties and disturbances; in the second phase, we have flexibility in designing the velocity profile

The paper is organized as follows: in section II, we introduce the underlying assumptions of this work, and several concepts and remarks that are important in understanding the algorithm. In section III, we formulate the first phase delay and reroute integer programming model, and talk about some additional modeling considerations. In section IV, we propose the second phase model to optimize speed profile given geofence location inputs from the first phase result. In section V, we summarize the findings and contributions of this paper, and point out the future work.

II. Model Assumptions and Preliminary Concepts

A. Model Assumptions

1) Airspace has structure (routes and waypoints), and the structure is given as parameters to the models. A waypoint can correspond to a physical landmark like a vertipad or ground surveillance station, or simply where routes cross each other. Flights are only allowed to fly on the routes
2) There can be multiple lanes corresponding to a route. Particularly, aircraft moving in opposite directions on a route will use different lanes. Therefore head-on collision is not considered
3) There is dynamic geofence associated with each flight. The dimension of the dynamic geofence is predetermined. The size of accessible region (blue region in Figure 1) is in general dependent on the flight operation, aircraft performance, on-board and ground Communication Navigation Surveillance equipments, etc. Since the aircraft is restricted to fly on the route, hence we only consider the length of the dynamic geofence and ignore its width and height
4) A flight operator is required to submit flight plan for each operation. We adopt the First Come First Serve (FCFS) policy and will *sequentially* submit and process flight plans. Therefore, when we plan a trajectory for the current flight, all information about the previous flight plans and allocated airspace is known
5) Flights with different onboard equipment and aircraft performance will fly in different layers. We focus on 2-dimensional airspace and en route phase
6) The model is discretized into time periods of equal size

Fig. 1 Illustration of Dynamic Geofence

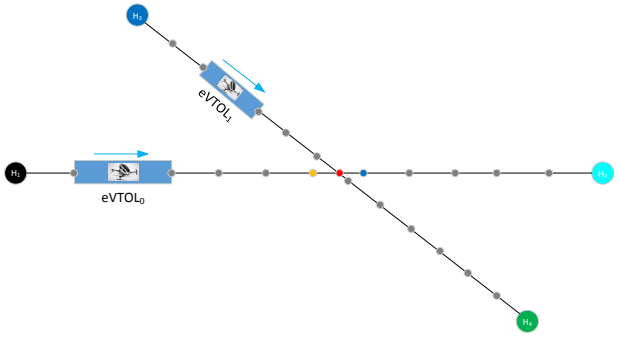

Fig. 2 Illustration of Discretization

B. Preliminary Concepts and Remarks

1. Model Discretization, Time Period, Dynamic Geofence

Assume the cruise speed of an eVTOL is 30m/s, the distance between vertipad A to waypoint B is 9km. If the length of a time period is 10 seconds, it will take 30 time periods for a flight to fly from A and reach B.

A "full" dynamic geofence is composed of an accessible region for enclosed aircraft and the region reserved to satisfy minimum separation requirement. We will only focus on the accessible region, because once we know geofences of all previously filed flights and the minimum separation requirement, we will know all of the constraints on the location of accessible regions. With slight abuse of terminology, we sometimes refer the accessible region as the dynamic geofence (for the enclosed aircraft).

If the length of dynamic geofence is 600m, it will take 2 time periods for this geofence to pass any point. We can envision that the dynamic geofence, which encloses the aircraft, is moving on a gridded route. At each timestamp, it occupies three grids, as shown in Figure 2. We do not restrict all flights to have the same constant cruise speed. If two flights have different speeds, the distance between two consecutive discretization points will differ.

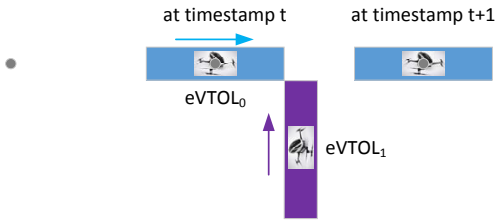

Fig. 3 Collision During Two Timestamps

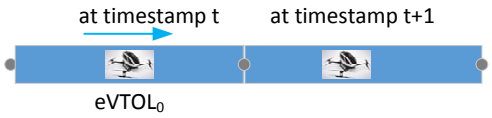

Fig. 4 Union of Two Consecutive Geofences

2. Union of Dynamic Geofences

It is important to note that even if two dynamic geofences do not have conflict at two discrete timestamps, they can have conflict during these two timestamps, as shown in Figure 3. In order to guarantee there is no conflict during $[t_{i-1}, t_i]$, we ensure that the geofence at t_{i-1} is connected with geofence at t_i, and we set $\mathrm{DG}_{f,[t,t+1]} = \mathrm{DG}_{f,t} \bigcup \mathrm{DG}_{f,t+1}$. For example, in Figure 4 the dynamic geofence is one time period long. Even though the geofence may leave the left node immediately after timestamp t, but we will reserve the left node for eVTOL_0 during the whole time period $[t, t+1]$. Consequentially, later filed aircraft cannot access the airspace region between the left node and right node during $[t, t+1]$. In this paper, we let time period to start from 1 and call $[t, t+1]$ time period $t+1$.

3. Three Dimensional Routes, Vertical Maneuvers, Capacity of Potential Collision Node

The Dynamic Skylane Networks concept proposed by Uber is essentially a 3-dimensional route (tube) [4, 22]. By leveraging the altitude dimension, it is possible to avoid intersections and potential collision points in many regions. However, as the number of vertipads and routes increase, it is possible at certain places, route crossing at the same

altitude is inevitable. In that case, we can apply the algorithm proposed in this paper. In this sense, this work is compatible with concept and roadmap advocated by Uber.

In this work, we assume aircraft avoid collision by rerouting or taking delay. It is possible that aircraft can perform vertical or 3-dimensional maneuvers, like resolution solution generated from NASA AutoResolver. We can argue that while it is easy for two flights to do this kind of "local" maneuver to avoid collision, it can be tricky for three or even more flights to maneuver and do conflict resolution at one potential collision point. A way to account for the possibility of local maneuver is that we can think that certain potential collision points have capacity, which equals to maximum number of flights allowed to do maneuver and pass through that point. If needed, we can add one or more units of air delay to flight to account for extra maneuver time.

4. Two Possible Structured Airspace Designs

There can be two possible structured airspace designs: locally connected structured airspace, shown in the left of Figure 5, and densely connected network, shown in the left of Figure 5. For locally connected network, it resembles the jet routes and waypoints in high-altitude airspace. The main advantage of this design is that the structure is relatively simple and there are fewer intersections (potential collision points). The disadvantage of such design is that even for a short haul flight, aircraft has to fly on the route and sometimes this results in a zigzag route.

For low altitude UAM operation in which flight endurance is a concern, it is argued by many people that direct route between vertipads is more preferable. In this densely (fully or near fully) connect case, there will be a lot more potential collision points. Thus the trajectory planning algorithm has to be scalable. In the next two sections, we will talk about how we are able to use linear programming tools, which are highly scalable, to solve this problem.

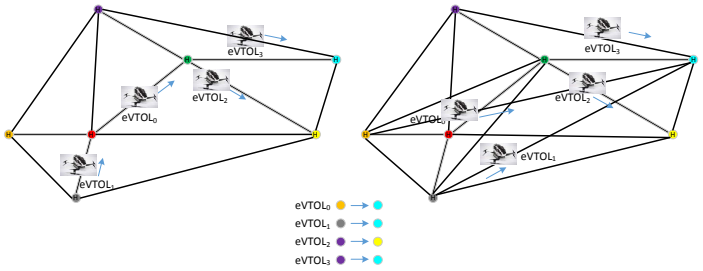

Fig. 5 Illustration of Two Structured Airspace Designs

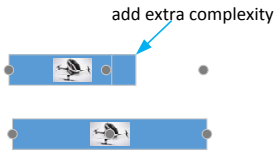

Fig. 6 Geofence Bounded by Grid Points

III. Sequential Trajectory Planning in Time-space Network

In this section, we talk about how to plan a conflict free trajectory for dynamic geofence in a densely connected network. Note that if we allow a flight to freely reroute in this type of network, the number of decision variables can be enormous. If we restrict the flight to fly only on the direct /shortest route, the flight would have too little freedom and it would be a waste of airspace resources. Hence, we borrow the ideas from Collaborative Trajectory Options Program (CTOP) [23], and allow the flight to choose a route from a set of predetermined reroute options between two vertipads. For each reroute option, all we need to do is to manage aircraft to pass potential collision points along the route without conflict.

A. Preprocessing Filed Flight Plans

To facilitate data preprocessing, we require the boundary of dynamic geofence to be bounded by grid points, as shown in Figure 6. That means, when the spaces between grid points are not exactly the same, the length of dynamic geofence can be slightly different.

The goal of preprocessing filed flight plan is to figure out that for potential collision points, which are the accessible time periods for the current flight. Because we plan flight one at a time, therefore M_t^p in constraint (7) is binary parameter. For example, if dynamic geofence is 2 time periods "long" (occupies three nodes as shown in Figure 2), because we need to consider the union operation (section II.B.2), only if potential collision point p *has capacity* at time periods $t, t+1, t+2, t+3$, we set $M_t^p = 1$.

When we do discretization along the route, it is most likely that a potential collision point does not coincide with any

discretization point. In Figure 2 for eVTOL$_0$, the potential collision point is in between two discretization points (painted in orange and blue). If a potential collision point is *occupied* in time periods t and $t+1$, for the discretization point colored in blue, considering that the geofence is 2 time periods "long", we will need to set $M^p_{t-2} = M^p_{t-1} = M^p_t = M^p_{t+1} = 0$.

B. Model Formulation

We propose a binary integer formulation based on Bertsimas-Stock model [24, 25], which is known to be a strong formulation:

$$\min \quad \sum_{r\in\mathcal{F}_f}\left[\left(c_{fr}-(c_g-c_a)\mathrm{Dep}_f-c_a\mathrm{Arr}_f\right)\delta_{fr}+(c_g-c_a)\sum_{t\in T^p_{fr};p=\Omega^0_{fr}} t(w^p_{fr,t}-w^p_{fr,t-1})+c_a\sum_{t\in T^p_{fr};p=\Omega^{N_{fr}}_{fr}} t(w^p_{fr,t}-w^p_{fr,t-1})\right] \tag{1}$$

$$w^{pr}_{f,\underline{T}^p_{fr}-1} = 0 \qquad r\in\mathcal{F}_f, p\in\Omega_{fr} \tag{2}$$

$$w^{pr}_{f,\overline{T}^p_{fr}} = \delta_{fr} \qquad r\in\mathcal{F}_f, p=\Omega^0_{fr} \tag{3}$$

$$\sum_{r\in\mathcal{F}_f}\delta_{fr} = 1 \tag{4}$$

$$w^{p'r}_{f,t+\Delta^{p,p'}} - w^{pr}_{f,t} \le 0 \qquad \forall r\in\mathcal{F}_f, p,p'\in\Omega_{fr},(p,p')\in C, t\in T^p_{fr} \tag{5}$$

$$w^{pr}_{f,t} - w^{pr}_{f,t-1} \ge 0 \qquad \forall r\in\mathcal{F}_f, p\in\Omega_{fr}, t\in T^p_{fr} \tag{6}$$

$$\sum_{(f,r)\in\Phi_p;t\in T^p_{fr}}(w^p_{frt} - w^p_{fr,t-1}) \le M^p_t \qquad \forall r\in\mathcal{F}_f, p\in\Omega_{fr}, t\in\mathcal{T} \tag{7}$$

$$g_f = \sum_{r\in\mathcal{F}_f}\left[\sum_{t\in T^p_{fr};p=\Omega^0_{fr}} t(w^p_{fr,t} - w^p_{fr,t-1}) - \delta_{fr}\mathrm{Dep}_f\right] \tag{8}$$

$$a_f = \sum_{r\in\mathcal{F}_f}\left[\sum_{t\in T^p_{fr};p=\Omega^{N_{fr}}_{fr}} t(w^p_{fr,t} - w^p_{fr,t-1}) - \delta_{fr}\mathrm{Arr}_f\right] - g_f \tag{9}$$

Constraints (2) are the boundary conditions. Constraints (3)-(4) impose that one and only one route should be chosen for this flight. Constraints (5) represent the connectivity in two potential collision points. Constraints (6) model the connectivity in time. Constraints (7) are the capacity constraints at each possible collision point.

Equations (8) and (9) give the expressions for ground delay and air delay, respectively. The objective function is composed of three parts: the ground delay cost, air delay cost and route cost. Route cost c_{fr} can account for total flight time, battery consumption, and even congestion fee if airspace regulator charges it.

C. Limiting the Amount of Delay

The parameter T directly controls the maximum delay flight f is allowed to take. By setting $\bar{T}^{p=\Omega^0_{fr}}_{fr}$ as a small number, we can limit the amount of allowed ground delay.

When two potential collision points are very close to each other, it is not realistic for a flight to take even one unit of air delay. In that case, for such (p,p') on route r we can impose that

$$w^{p'r}_{f,t+\Delta^{p,p'}} - w^{pr}_{f,t} = 0 \quad t\in T^p_{fr} \tag{10}$$

In general, if the maximum air delay between (p,p') on route r is $d_{p,p'}$, we can add the following set of constraints:

$$w^{p'r}_{f,t+\Delta^{p,p'}+d^{p,p'}} - w^{pr}_{f,t} \ge 0 \quad t\in T^p_{fr} \tag{11}$$

D. Formulation Properties

There are three differences between the formulation in this paper and the original formulation in [24]. First, this is no longer a multi-commodity flow model because we plan flights sequentially. Second, even though a flight can have multiple route options, since they are not coupled, we can evaluate route options in parallel. Third, we do not consider the connectivity constraint between flights at a vertipad, which was used in [24] several times to construct counterexamples and prove that certain good properties, in general, do not hold. As a result, the formulation is not just a strong formulation, but a perfect formulation.

Theorem 1 *Sequential delay and reroute binary linear formulation (1)-(11) is Totally Unimodular (TU).*

Proof: Since each route option can be evaluated separately, there is no need to do the summation in (4) and (7). Consequently, for each constraint in the formulation, there are at most two decision variables. Whenever there are two decision variables, one is associated with the positive sign and the other is associated with the negative sign. Thus the dual form of the coefficient matrix is a *network matrix* [26]. Since the network matrix is a sufficient condition for TU, hence the formulation is TU. □

Corollary 1.1 *Whenever linear relaxation of this binary linear formulation has a finite optimal solution, it has an integral optimal solution.*

We give a concrete example in appendix VI.A to show the pattern of coefficient matrix.

In this formulation, δ_{fr} are introduced only for the purpose of making the model more readable. The number of decision variables $w_{f,t}^{pr}$ is $\sum_{r\in\mathcal{F}_f}\sum_{p\in\Omega_{fr}}|T_{fr}^{p}|$. The number of constraints is at most $\Big(\sum_{r\in\mathcal{F}_f}\sum_{p\in\Omega_{fr}}1\Big)+1+2\sum_{r\in\mathcal{F}_f}\sum_{p\in\Omega_{fr}}|T_{fr}^{p}|+\sum_{r\in\mathcal{F}_f}\sum_{p\in\Omega_{fr}}T$

E. Remarks and Additional Model Considerations

1. Length of Dynamic Geofence and Time Period, Aircraft Performance

The first two important decisions we need to make are the length of the dynamic geofence and the length of a time period (mesh size). As discussed in section II.B.2, the basic requirement is that we want the dynamic geofence at two consecutive time periods to be connected (head-tail linked). Therefore, if the length of the dynamic geofence is first given, then it will impose an upper bound on the length of a time period. We do not want the length of a time period to be too small. Otherwise, it will take longer time to do data preprocessing and it will generate a lot of constraints for speed profile smoothing problem, which will be discussed in section IV.

The length of the dynamic geofence is related to the aircraft performance. Let us continue the example in II.B.1. If a flight takes one unit of air delay, the geofence will stop moving for 10 seconds. If the aircraft happens to be in the middle of the dynamic geofence, because the dynamic geofence is two time periods long, the aircraft in theory can keep flying without changing speed. If so, it will now be at the front end of the dynamic geofence. Eventually we need to change the speed so that the flight is back to the desired location (center or close to rear end in order to absorb delay in the future). In this case, the geofence will serve as a buffer zone for the enclosed aircraft to do speed adjustment.

In practice, to make the trajectory flyable, after deciding the amount of the air delay between each potential collision point, we need to smooth and refine the speed profile and let the aircraft always near the desired location of the dynamic geofence. It can be seen that an aircraft with better acceleration and deceleration performance and a longer dynamic geofence can both make the speed profile design task easier. Hence there is a tradeoff here: a long dynamic geofence allows aircraft to do more en route air delay, and potentially could save very long ground delay. On the other hand, a long dynamic geofence will occupy more airspace resource and can potentially make other flights take longer delay.

2. Space Between Two Consecutive Flights

In general we do not need to worry about the spacing between two consecutive flights on the same route. Because we can control the amount of allowable air delay, and we can assume (control) the departure times between two flights is far enough from each other.

If we have to consider the dynamic geofence conflict between two consecutive flights, not only the crossing points between routes, but all discretization points along the route can be potential collision points.

3. Local Maneuvers

As mentioned in section II.B.3, if we allow aircraft to perform maneuvers to avoid collision, then it is possible that more than one aircraft are crossing the potential collision point in the same time period. If we assume the extra time needed to perform maneuvers is negligible, we only need to consider the capacity of the node when we do the flight plan pre-processing, the formulation will stay the same.

The interesting case is when doing a maneuver takes one or more time periods to finish. For Figure 2, we mentioned in section III.A that by setting the capacity of the blue point to be 0, we can avoid the conflict at the potential collision point (red node). If $T_{fr}^{p'} = \{7, 8, 9, 10, 11, 12, 13, 14\}, \tilde{T}_{fr}^{p'} = \{11, 12\}$, where p' is the blue point. If $\Delta^m = 1$, the geofence is 2 time periods "long", and we decide to let the aircraft to perform local maneuvers in face of congestion, we can impose:

$$w_{f,t+2}^{p'r} - w_{f,t}^{pr} = 0 \qquad t \in \{8, 9, 10, 11\} \tag{12}$$

$$w_{f,t+1}^{p'r} - w_{f,t}^{pr} = 0 \qquad t \in \{6, 7, 12, 13\} \tag{13}$$

That is to say, if the front end geofence reaches orange node in time period 7, it will reach the blue node in time period 8. The entire geofence can pass the blue node without doing maneuver and without any confliction. If the geofence reaches orange node in time period 8, it will need to do the maneuver, which takes one time period. Because if it does not do so, in time period 11 its rear end will have conflict with other aircraft at the blue node.

4. On-demand Vs. Scheduled Operation, Impact on System Cost

If we know all of the demand between vertipads before the day of operation, in theory we can do centralized offline scheduling for multiple flights at a time. It is expected that in this case, the system wide cost can be notably reduced. For example, now we can use larger delay cost coefficients for important flights to give them higher priority in using airspace resources. However, in this case we will need to deal with the multi-commodity flow problem. For a given flight, the route can no longer be evaluated separately in parallel. Discretization step can also be trickier to do. In summary, it is more difficult to use the current framework to deal with collision voidance for multiple aircraft in batch.

IV. Speed Profile Smoothing

1. Model Formulation

In this section, we talk about how to optimize the speed profile after solving the first phase problem in the previous section. Now L_t, R_t and o_t are now known values and will be the input parameter to the problem in this section. We use a finer-grained time discretization, e.g. 0.2 sec or 0.5 sec, which is close to the value of a guidance cycle. We use $\bar{t}$ here to differentiate the time period t used in III.B. The formulation is shown below:

$$\min \quad \alpha \sum_{t \in \mathcal{T}} \|x_t - o_t\| + \sum_{\bar{t} \in \bar{\mathcal{T}}} \left(\beta \|a_t\| + |a_{\bar{t}+1} - a_{\bar{t}}| \right) \tag{14}$$

$$x_{\bar{t}+1} = x_{\bar{t}} + v_{\bar{t}} \Delta \bar{t} \qquad \bar{t} \in \bar{\mathcal{T}} \tag{15}$$

$$v_{\bar{t}+1} = v_{\bar{t}} + a_{\bar{t}} \Delta \bar{t} \qquad \bar{t} \in \bar{\mathcal{T}} \tag{16}$$

$$L_t \le x_t \le R_t \qquad t \in \mathcal{T} \tag{17}$$

$$v_{\min} \le v_{\bar{t}} \le v_{\max} \qquad \bar{t} \in \bar{\mathcal{T}} \tag{18}$$

$$a_{\text{dec}} \le a_{\bar{t}} \le a_{\text{acc}} \qquad \bar{t} \in \bar{\mathcal{T}} \tag{19}$$

$$|a_{\bar{t}+1} - a_{\bar{t}}| \le \dot{a}_{\max} \Delta \bar{t} \qquad \bar{t} \in \bar{\mathcal{T}} \tag{20}$$

Constraints (15)-(16) are the location and velocity updates using Euler's method. Constraints (18)-(20) impose bounds on velocity, acceleration, jitter, respectively. We only know the location of L_t, R_t when $t \in \mathcal{T}$. Constraints (17) ensure that at these timestamps, the aircraft is in the dynamic geofence. Because we design consecutive dynamic geofences to be connected and we take union operation to reserve airspace resource, the aircraft is always kept in the geofence.

Once L_t and G_t is known, o_t can be easily determined. The first term in the objective function penalizes the deviation from desired location; the second term penalizes the battery usage; the third term penalizes passenger discomfort. α and

β are weighting coefficients. Depending on the norms used in the objective function, this formulation can be a linear programming or quadratic programming problem. Either case can be very efficiently solved.

2. Handle Local Maneuver

In section 7, we talked about the possibility of an aircraft performing local maneuvers to share a potential collision node with another aircraft. When performing maneuvers, it can take aircraft more than one time period to reach next discretization node. It is important to see that the geofence does not stop moving, which is different from taking air delay. In the speed profile smooth formulation, we can add *artificial intermediate nodes* between two discretization nodes to account for the fact that the geofence has been moving but it takes longer time to reach the next discretization point. Before solving the speed smoothing problem, we also need to adjust the values of L_t (and corresponding R_t) for

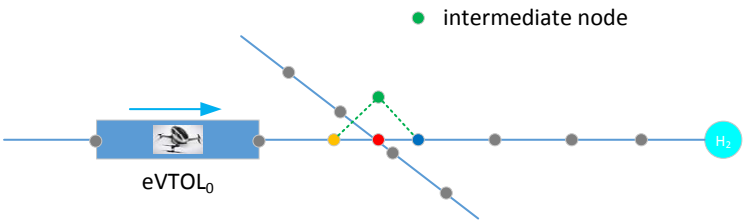

Fig. 7 Illustration of Artificial Intermediate Node and Arcs

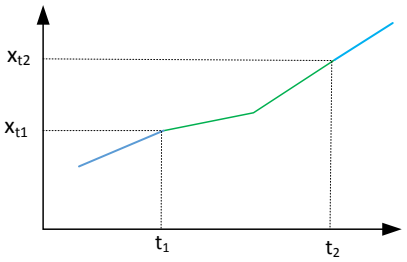

Fig. 8 Illustration of the Solution

these L_t which exceed the the coordinate value of the orange node.

Figure 8 shows an illustration of the solution. Since we know the distance from the departure vertipad to the orange node x_{t_1}, we know this aircraft will reach orange node at t_1. We also know the length of these two artificial arcs, hence we know this aircraft will reach the blue node at t_2. For $t \leq t_1, t \geq t_2$, the aircraft is flying along the route.

V. Conclusions

In this paper, we proposed a two-phase optimization based pre-departure trajectory planning algorithm. We find that if we sequentially process and plan a trajectory for each aircraft, the conflict avoidance integer programming formulation is TU, which allows us to solve it using linear programming. This pre-departure planning algorithm can bring three major benefits:

1) verifiable safety guarantee, since any feasible solution satisfies all the separation and operation constraints
2) strategic decisions, including how long should the flight be held on the ground to avoid congestion, which route (direction) should be chosen, etc
3) predictability, since a flight is restricted in the dynamic geofence and the location of the dynamic geofence is known after solving the model. More over, we know at which section of the path the speed adjustment is expected, etc

Due to the listed benefits, we believe the concept of dynamic geofence and, especially, pre-departure planning can play an important role in future UAM operations. In future work, we will test our algorithm on realistic use cases.

VI. Appendix

A. Pattern of Coefficient Matrix

In the following example, there are two possible collision points. The travel time between vertipad and first potential collision point, and between potential collision points are both 2 time periods. Let $T = 8, T^0_{fr} = \{0, 1, 2, 3\}, T^1_{fr} = \{2, 3, 4, 5\}, T^2_{fr} = \{4, 5, 6, 7, 8\}$, scheduled departure time is $t = 1$, maximum units of air delay between potential collision point is 1. The coefficient matrix is listed in Table:

There are six block of rows in Table 1. The first three block of rows correspond to constraints (2), (6) and (7); the fourth and fifth block of rows correspond to constraints (5); the last block of rows correspond to constraints (11).

$w^{0r}_{f,0}$	$w^{0r}_{f,1}$	$w^{0r}_{f,2}$	$w^{0r}_{f,3}$	$w^{1r}_{f,2}$	$w^{1r}_{f,3}$	$w^{1r}_{f,4}$	$w^{1r}_{f,5}$	$w^{2r}_{f,4}$	$w^{2r}_{f,5}$	$w^{2r}_{f,6}$	$w^{2r}_{f,7}$	$w^{2r}_{f,8}$
1												
-1	1											
	-1	1										
		-1	1									
			1									
				1								
				-1	1							
					-1	1						
						-1	1					
								1				
								-1	1			
									-1	1		
										-1	1	
											-1	1
	-1				1							
		-1				1						
			-1				1					
					-1				1			
						-1				1		
							-1				1	
					-1					1		
						-1					1	
							-1					1

Table 1 Coefficient Matrix of a Small Example

VII. Acknowledgement

The authors would like to gratefully acknowledge Richard Golding and Peter Sachs at Airbus A^3 for their helpful discussions in the early stages of this research. The authors also benefit from the discussions with Marc Brittain and Xuxi Yang.

References

[1] Uber Elevate, "Fast-Forwarding to a Future of On-Demand Urban Air Transportation," 2016.

[2] Gipson, L., "NASA Embraces Urban Air Mobility, Calls for Market Study," `https://www.nasa.gov/aero/nasa-embraces-urban-air-mobility`, Nov. 2017. Acessed Nov 20, 2018.

[3] Airbus, "Urban Air Mobility by Airbus, Airbus Information," 2018.

[4] Uber Elevate, "Airspace Management at Scale: Dynamic Skylane Networks," 2nd Annual Uber Elevate Summit, 2018.

[5] Mueller, E. R., Kopardekar, P. H., and Goodrich, K. H., "Enabling Airspace Integration for High-Density On-Demand Mobility Operations," *17th AIAA Aviation Technology, Integration, and Operations Conference*, 2017, p. 3086.

[6] Vascik, P. D., "Systems-level analysis of On Demand Mobility for aviation," Master's thesis, Massachusetts Institute of Technology, 2017.

[7] Erzberger, H., "Automated conflict resolution for air traffic control," *25th International Congress of the Aeronautical Sciences*, 2005.

[8] Erzberger, H., Lauderdale, T., and Chu, Y., "Automated conflict resolution, arrival management, and weather avoidance for air traffic management," *Proceedings of the Institution of Mechanical Engineers, Part G: Journal of aerospace engineering*, Vol. 226, No. 8, 2012, pp. 930–949.

[9] Erzberger, H., Nikoleris, T., Paielli, R. A., and Chu, Y.-C., "Algorithms for control of arrival and departure traffic in terminal airspace," *Proceedings of the Institution of Mechanical Engineers, Part G: Journal of Aerospace Engineering*, Vol. 230, No. 9, 2016, pp. 1762–1779.

[10] Bosson, C., and Lauderdale, T. A., "Simulation Evaluations of an Autonomous Urban Air Mobility Network Management and Separation Service," *2018 Aviation Technology, Integration, and Operations Conference*, 2018, p. 3365.

[11] Muñoz, C., Narkawicz, A., Hagen, G., Upchurch, J., Dutle, A., Consiglio, M., and Chamberlain, J., "DAIDALUS: detect and avoid alerting logic for unmanned systems," *2015 IEEE/AIAA 34th Digital Avionics Systems Conference (DASC)*, IEEE, 2015, pp. 5A1–1.

[12] Schouwenaars, T., De Moor, B., Feron, E., and How, J., "Mixed integer programming for multi-vehicle path planning," *2001 European Control Conference (ECC)*, IEEE, 2001, pp. 2603–2608.

[13] Ong, H. Y., and Kochenderfer, M. J., "Markov decision process-based distributed conflict resolution for drone air traffic management," *Journal of Guidance, Control, and Dynamics*, 2016, pp. 69–80.

[14] Yang, X., and Wei, P., "Autonomous On-Demand Free Flight Operations in Urban Air Mobility using Monte Carlo Tree Search," International Conference on Research in Air Transportation (ICRAT), Barcelona, Spain, 2018.

[15] Brittain, M., and Wei, P., "Autonomous Air Traffic Controller: A Deep Multi-Agent Reinforcement Learning Approach," *arXiv preprint arXiv:1905.01303*, 2019.

[16] Zhu, G., and Wei, P., "Low-Altitude UAS Traffic Coordination with Dynamic Geofencing," *16th AIAA Aviation Technology, Integration, and Operations Conference*, 2016, p. 3453.

[17] Stevens, M. N., and Atkins, E. M., "Geofencing in Immediate Reaches Airspace for Unmanned Aircraft System Traffic Management," *2018 AIAA Information Systems-AIAA Infotech@ Aerospace*, 2018, p. 2140.

[18] Lee, J., Hwang, I., and Shim, D. H., "UAS Surveillance in Low-altitude Airspace with Geofencing: Constrained Stochastic Linear Hybrid Systems Approach," *2018 AIAA Information Systems-AIAA Infotech@ Aerospace*, 2018, p. 0077.

[19] Federal Aviation Administration, "Near Midair Collision Reporting," `http://www.faraim.org/aim/aim-4-03-14-530.html`, 2017. Acessed April 20, 2019.

[20] Hoekstra, J. M., Ellerbroek, J., Sunil, E., and Maas, J., "Geovectoring: Reducing Traffic Complexity to Increase the Capacity of UAV airspace," *International Conference for Research in Air Transportation, Barcelona, Spain*, 2018.

[21] Hunter, G., and Wei, P., "Service-oriented separation assurance for small UAS traffic management," *Integrated Communication, Navigation and Surveillance technologies (ICNS), Herndon, VA*, 2019.

[22] Norris, G., "Uber Boosted By FAA's Openness To 'Skylane' UAM Routing Concept," *Aviation Week & Space Technology*, 2019.

[23] Zhu, G., and Wei, P., "An Interval-based TOS Allocation Model for Collaborative Trajectory Options Program," 2018. AIAA Aviation, Atlanta, GA.

[24] Bertsimas, D., and Patterson, S. S., "The air traffic flow management problem with enroute capacities," *Operations Research*, Vol. 46, No. 3, 1998, pp. 406–422.

[25] Bertsimas, D., Lulli, G., and Odoni, A., "An integer optimization approach to large-scale air traffic flow management," *Operations Research*, Vol. 59, No. 1, 2011, pp. 211–227.

[26] Nemhauser, G. L., and Wolsey, L. A., *Integer and combinatorial optimization*, John Wiley & Sons, 1988.